Electronic Supplementary Material (ESI) for Journal of Materials Chemistry A.
This journal is © The Royal Society of Chemistry 2014

Supporting Information

3D Hybrid of Layered MoS_2/Nitrogen-Doped Graphene Nanosheet Aerogels: an Effective Catalyst for Hydrogen Evolution in Microbial Electrolysis Cells

Yang Hou[a,§] Bo Zhang,[b,§] Zhenhai Wen,[a] Shumao Cui,[a] Xiaoru Guo,[a] Zhen He,[c,*] and Junhong Chen[a,*]

[a] Department of Mechanical Engineering, University of Wisconsin-Milwaukee, 3200 North Cramer Street, Milwaukee, Wisconsin 53211, USA

[b] Key Laboratory of Environmental Biotechnology, Research Center for Eco-Environmental Sciences, Chinese Academy of Science, Beijing 100085 China

[c] Department of Civil and Environmental Engineering, Virginia Polytechnic Institute and State University, Blacksburg, VA 24061, USA

[§]These authors have contributed equally.

* E-mail: zhenhe@vt.edu; jhchen@uwm.edu

Experimental Section

Synthesis of MoS_2-NS

Typically, 42 mg sodium molybdate and 84 mg thiourea were dissolved in 20 mL deionized water under vigorous stirring for 2 h to form a homogeneous solution. Subsequently, the resulting mixture was transferred to a Teflon-lined autoclave and heated at 210 °C for 24 h. Finally, a black product resulted, which was centrifuged and then washed with distilled water and ethanol before being dried at 60 °C in air overnight. Further exfoliation of MoS_2-NS into few-layer MoS_2-NS was completed by liquid exfoliation of obtained MoS_2-NS via sonication in mixed isopropyl alcohol/water.[1] 50 mg MoS_2-NS and 40 mL isopropyl alcohol/water (50 vol.%) were added into a 100 mL beaker. The sealed beaker was sonicated for 10 h, and then the dispersion was centrifuged at 1,000 rpm for 20 min. After centrifugation, the supernatant (about three-fourths of the centrifuged dispersion) was collected by pipette. The mass remaining in the supernatant was estimated by drying and weighing the sediments in the centrifugal tube and about three-fifths of the starting material remained in the supernatant. That was to say, the as-obtained supernatant possessed a concentration of ~1 mg mL^{-1}. The final product (few-layer MoS_2-NS) was collected by centrifuging the supernatant at 10,000 rpm for 30 minutes, and then dried in a vacuum oven at 60 °C overnight.

Synthesis of 3D MoS_2/N-GAs

Firstly, the graphene oxide (GO) was synthesized through chemical exfoliation of graphite powders using a modified Hummers' method.[2, 3] In a typical synthesis of the 3D MoS_2/N-GAs, 20 mg few-layer MoS_2-NS was gradually added to the 20 mL GO solution (2.5 mg mL^{-1}). Then, the mixture solution was stirred magnetically, and 2 mL ammonia was gradually added to the mixture. After sonication for 1 h, the resulting stable suspension was then transferred to a Teflon-lined autoclave, and hydrothermally treated at 180 °C for 12 h. Finally, the as-prepared product was dried to obtain aerogels (3D MoS_2/N-GAs).

As a control experiment, N-GAs was prepared in the absence of MoS_2-NS via a similar procedure.

Characterization

The morphology and composition of the 3D MoS_2/N-GAs hybrid were characterized using

a Hitachi H 9000 NAR transmission electron microscope (TEM) and a Hitachi S-4800 field emission scanning electron microscope (FESEM) equipped with an energy-dispersive X-ray spectroscopy analyzer. Atomic force microscopy (AFM) was conducted using an Agilent Technology 5420 AFM with a cantilever (Nanosensors PPP-77 NCH). Powder X-ray diffraction (XRD) data was collected using a Scintag XDS 2000 X-ray powder diffractometer operating at 40 kV, 40 mA for Cu Kα radiation (λ = 1.5418 Å). Raman spectra were taken using a Raman spectrometer with a 633 nm laser excitation (Renishaw 1000B). X-ray photoelectron spectroscopy (XPS) was performed using HP 5950A with Mg Kα as the source and the C 1s peak at 284.6 eV as an internal standard. Typically, the XPS scanning was recorded by 12 scans for the surface survey. For the high-resolution N 1s XPS scans, the parameter above was adjusted to 128 scans to produce an optimum signal-to-noise ratio. The number of XPS scanning was increased to make the deconvolution more clearly. It has no influence on the evaluation of nitrogen and other elements due to the calculations of their contents based on XPS surface survey. Thermogravimetric analysis (TGA) was carried out using a TA SDT 2960 thermoanalyzer with a heating rate of 5 °C min^{-1} in air atmosphere. Nitrogen adsorption-desorption isotherm measurements were performed on a Micromeritics ASAP 2020 to study specific surface area. Before analysis, all samples were pretreated by degassing at 200 °C for 8 h to remove any adsorbed species.

Electrochemical Test

Electrochemical measurements were performed in a standard three-electrode glass cell on a CH Instruments 760D electrochemical workstation using a glassy carbon electrode (GCE) with various catalysts as the working electrode, a Pt wire as counter electrode, and an Ag/AgCl electrode as the reference electrode. 100 mM PBS (PH = 7, purged with pure Ar) was used as the electrolyte. For the fabrication of the working electrode, 5.0 mg of the as-synthesized catalyst was mixed with a 50 μL Nafion solution (5% Nafion in ethanol) and 450 μL deionized water. The mixture was sonicated and a 5.0 μL suspension was pipetted out and dropped onto a glassy carbon electrode with a diameter of 3 mm and then fully dried. Linear sweep voltammetry was carried out from -0.2 to -1.4 V (vs. Ag/AgCl) at 5 mV s^{-1} for the polarization curves and Tafel plots. The catalyst was cycled 20 times by CV until a stable CV curve was obtained before testing.

The electrochemical impedance spectroscopy (EIS) was carried out in the frequency range of 10^{-2} to 10^{5} Hz with an AC voltage amplitude of 5 mV in Ar-saturated 100 mM PBS.

RHE Conversion

HER (100 mM PBS, PH = 7): the electrode potential is reported in this work relative to the reversible hydrogen electrode (RHE) potential, which was converted from the Ag/AgCl electrode using: $E_{RHE} = E_{(Ag/AgCl)} + 0.6106$ V.

The Setup and Operation of Microbial Electrolysis Cell

A flat plate MEC was used in this experiment (Figure S10 and Scheme S1). The anode electrode was a 5 cm long carbon brush and the cathode electrode was carbon cloth loaded with different catalysts. Before loading, the carbon cloth was soaked in acetone overnight and heated under 350 ºC for 1 hour to remove the impurities. The anode chamber and cathode chamber had the same volume, which was 30 mL. The anode chamber and cathode chamber were separated by a piece of cationic ion exchange membrane (Membrane International, Inc., Ringwood, NJ, USA). During operation, the anolyte was recirculated between MEC and a reservoir using a peristaltic pump (Cole Parmer) at 60 mL min^{-1}. The catholyte was not recirculated or mixed during the experiment.

The anolyte contained (per liter of tap water): sodium acetate, 1 g; NH_4Cl, 0.15 g; NaCl, 0.5 g; $MgSO_4$, 0.015 g; $CaCl_2$, 0.02 g; KH_2PO_4, 0.53 g; K_2HPO_4, 1.07 g; yeast extract, 0.1 g; and trace element, 1 mL.[4] The catholyte was 100 mM PBS. At the beginning of each cycle, 200 mL of anode feed solution was filled into a reservoir and recirculated through the MEC, while 30 mL of catholyte was fed into the cathode chamber of the MEC. The MEC was powered by a power supply (3644 A, Circuit Specialists, Inc., Mesa, AZ, USA), and the resistance used in this experiment was 1 Ω. The voltage across the resistor was recorded every 5 min using a data acquisition system (2700, Keithley Instruments, Inc., Cleveland, OH, USA). The gas produced during the experiment was collected in a graduated cylinder by water replacement. The composition of the gas was analyzed using gas chromatography.

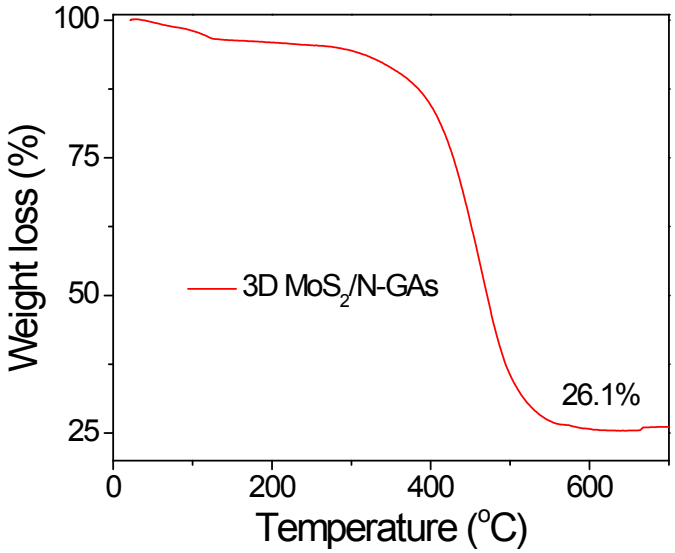

Figure S1. TGA curve of 3D MoS_2/N-GAs under flowing Air.

TGA analysis was employed to determine the content of MoS_2-NS present in the 3D MoS_2/N-GAs hybrid (Figure S1). Assuming that all MoS_2 was transferred to MoO_3 and all NG was burned out, the final residue was only MoO_3 after heating the composite to about 700 °C. Based on the mass of MoO_3 (26.1 wt.%) left after heating, it can be calculated that the MoS_2-NS content in the hybrid was about 29.0 wt.%.

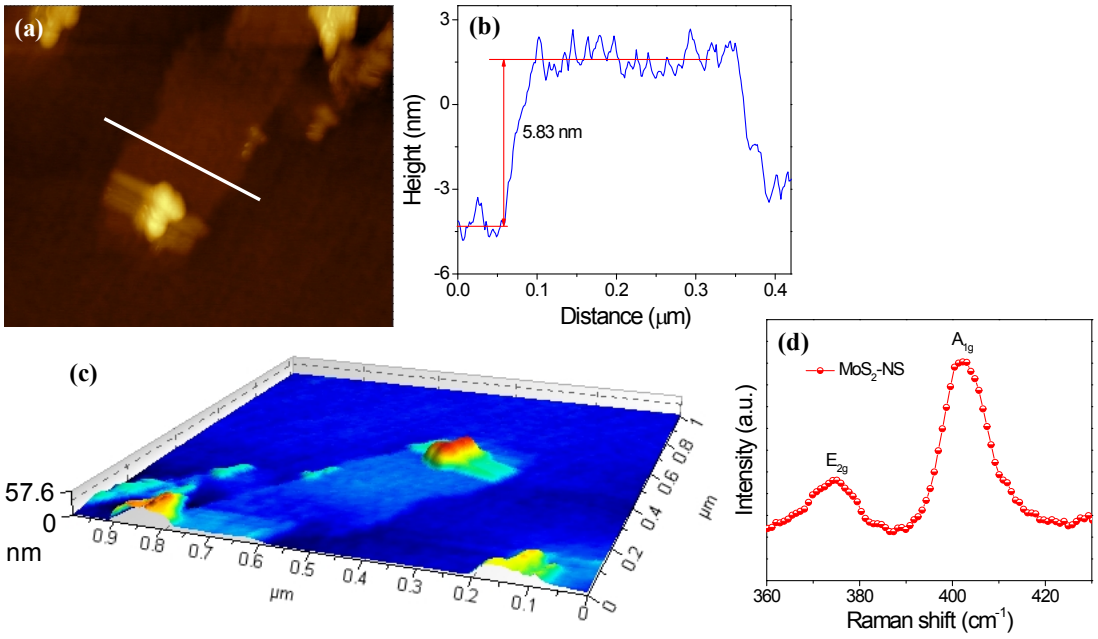

Figure S2. (a) AFM image of MoS_2-NS, (b) corresponding height profile of MoS_2-NS, (c) 3D AFM image from (a), and (d) Raman spectrum of MoS_2-NS.

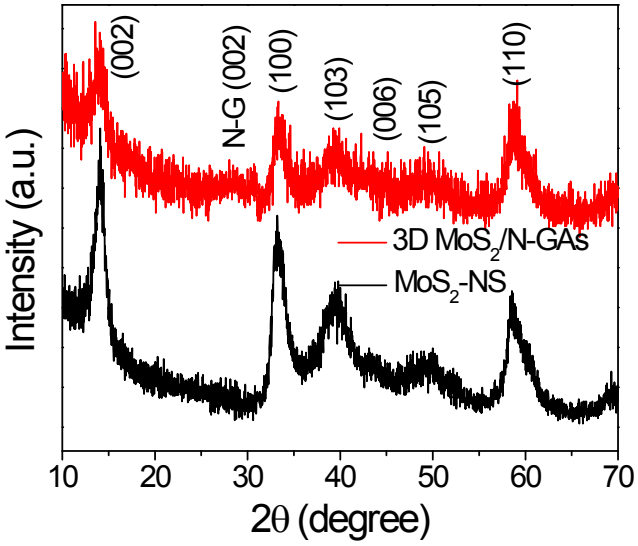

Figure S3. XRD patterns of MoS_2-NS and 3D MoS_2/N-GAs.

The 3D MoS_2/N-GAs hybrid displayed a similar crystalline structure to that of MoS_2-NS as shown in X-ray diffraction (XRD) patterns, which was congruent with a hexagonal structure (JCPDS 37-1492). The diffraction peaks at 14.1, 33.5, 39.4, 44.0, 49.8, and 58.9° corresponds to (002), (100), (103), (006), (105), and (110) crystal planes of MoS_2, respectively (Figure S3). A broad peak centered at 27.9° resulted from the NG nanosheets, revealing the co-existence of MoS_2-NS and N-GAs.

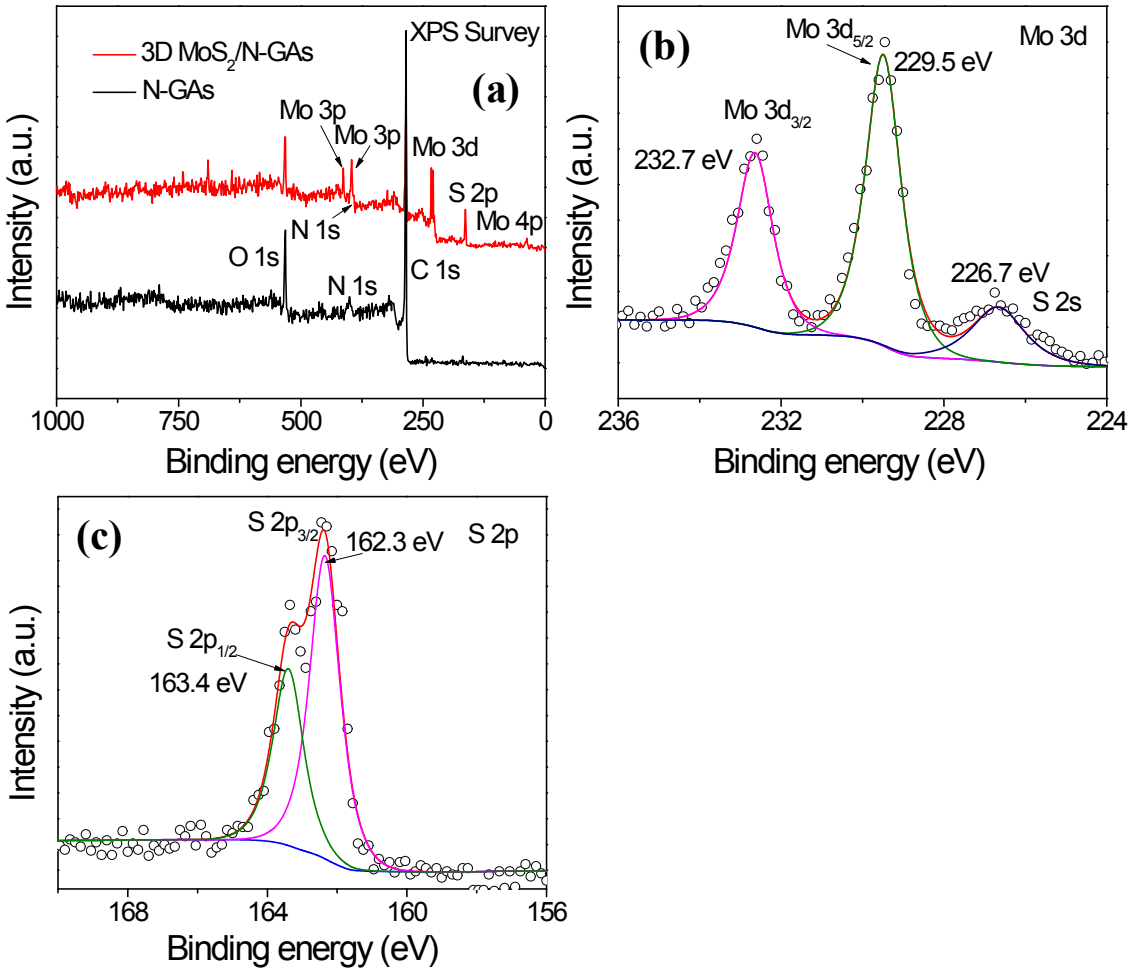

Figure S4. (a) The survey XPS spectra, (b) Mo 3d and, (c) S 2p XPS spectra for N-GAs and 3D MoS_2/N-GAs.

In Figure S4b, two peaks for the Mo 3d are observed at 229.5 and 232.7 eV, and assigned to Mo $3d_{5/2}$ and Mo $3d_{3/2}$, respectively. These values agree well with XPS data in the literature and are known to be due to Mo^{4+} species in the form of pure MoS_2.[5] The peak at 226.7 eV could be indexed as S 2s.[6] In addition, XPS peaks of S 2p located at 162.3 and 163.4 eV could be assigned to the spectra of S $2p_{3/2}$ and S $2p_{1/2}$ for S 2p (Figure S4c), which is in accordance with the sulfur element in the sulfides.[7]

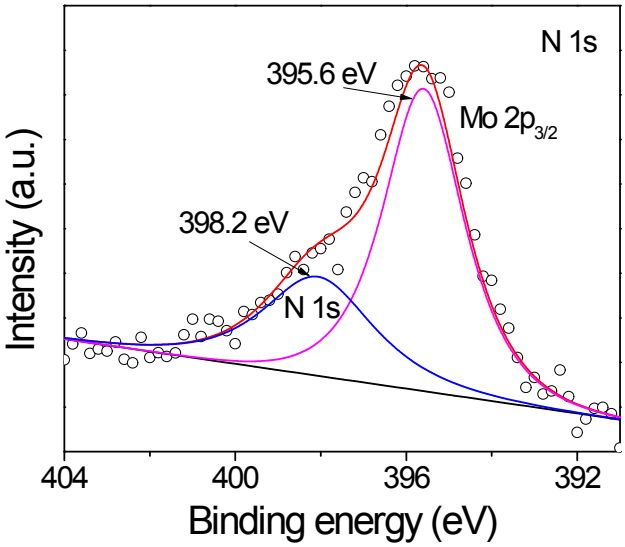

Figure S5. (a) High-resolution N 1s XPS spectrum of 3D MoS_2/N-GAs.

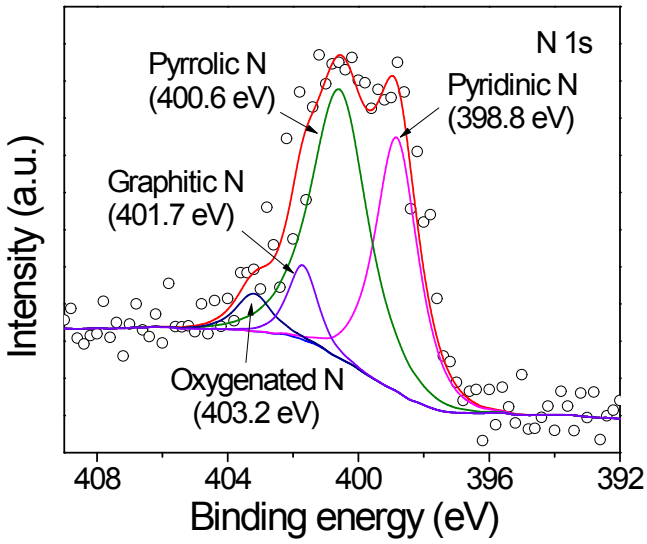

Figure S6. (a) High-resolution N 1s XPS spectrum of N-GAs.

In Figure S6, The complex N 1s spectra are deconvoluted into four peaks centered at 398.8, 400.6, 401.7, and 403.2 eV, corresponding with pyridinic N, pyrrolic N, graphitic N, and oxygenated N, respectively.[8]

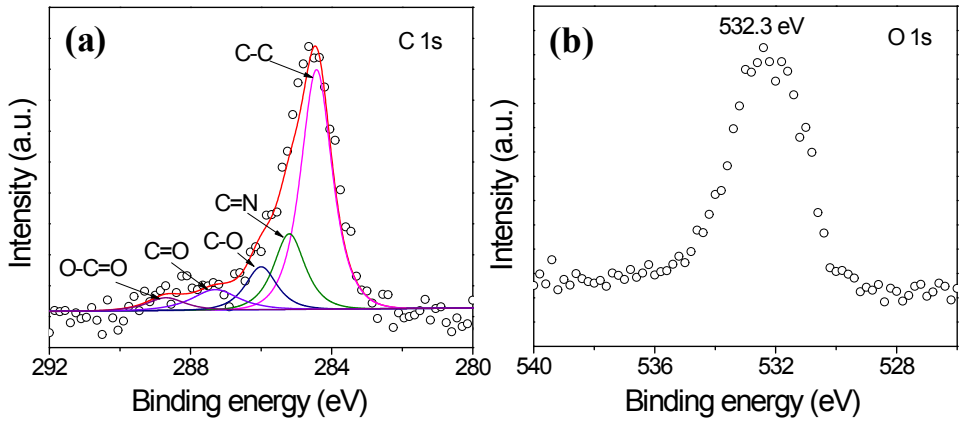

Figure S7. High-resolution C 1s (a) and O 1s (b) XPS spectra of 3D MoS_2/N-GAs.

The C 1s peaks for 3D MoS_2/N-GAs were deconvoluted into five peaks at 284.5, 285.2, 286.0, 287.4, and 288.7 eV, which are attributed to C–C, C=N, C–O, C=O, and O-C=O, respectively (Figure S7a).[9] The existence of C=N bonds undoubtedly verified the doping of N atoms within the hybrid. Nevertheless, the fact that there were still small amounts of oxygen in the hybrid (Figure S7a-S7b) suggests that most of the oxygen functional groups were removed during the hydrothermal processes.

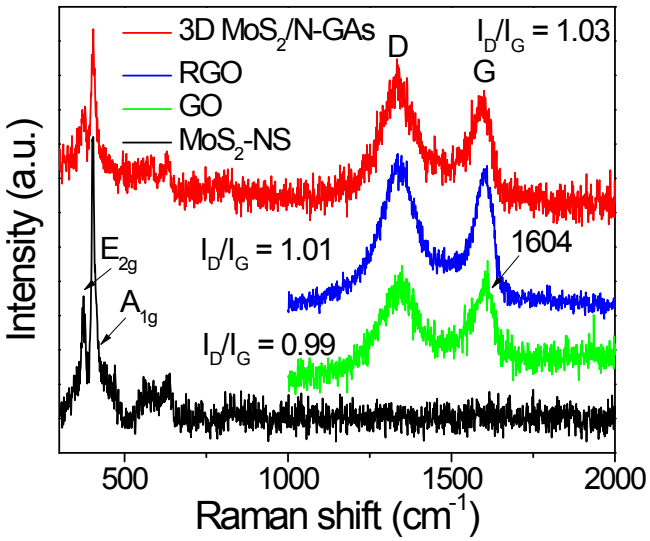

Figure S8. Raman spectra of MoS_2-NS, GO, RGO, and 3D MoS_2/N-GAs.

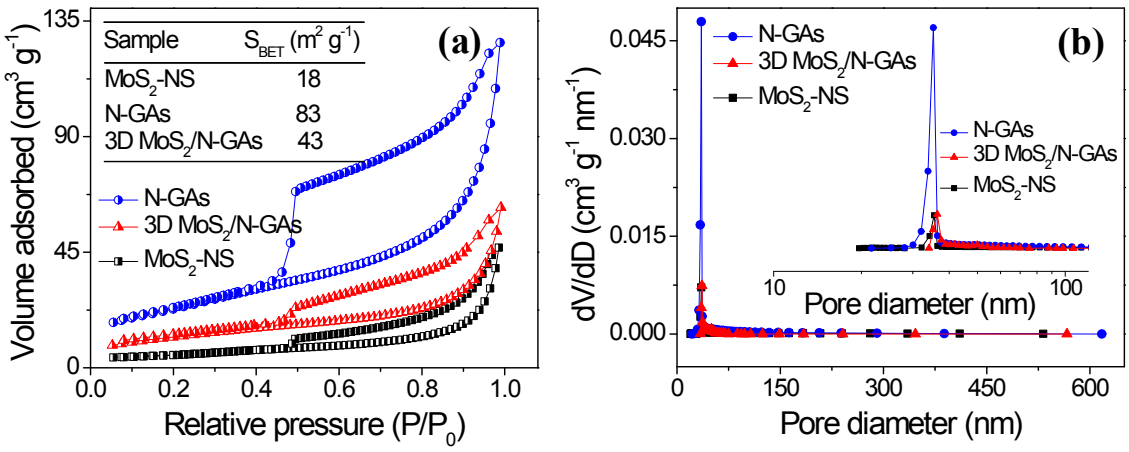

Figure S9. (a) The nitrogen adsorption-desorption isotherm and (b) the corresponding pore size distribution curves calculated from desorption branch of the nitrogen isotherm of MoS_2-NS, N-GAs, and 3D MoS_2/N-GAs.

The porous nature of the 3D MoS_2/N-GAs hybrid was characterized by measuring the nitrogen adsorption-desorption isotherm (Figure S9). A typical type IV isotherm with a H3 hysteresis loop demonstrates the mesoporous structure of the hybrid.[10] The obtained 3D MoS_2/N-GAs hybrid had a large Brunauer-Emmett-Teller (BET) surface area of 43 m^2 g^{-1} and the average pore size was about 71 nm, which is essential for diffusion of the electrolyte and increasing the contact between electrolyte and catalyst.[11]

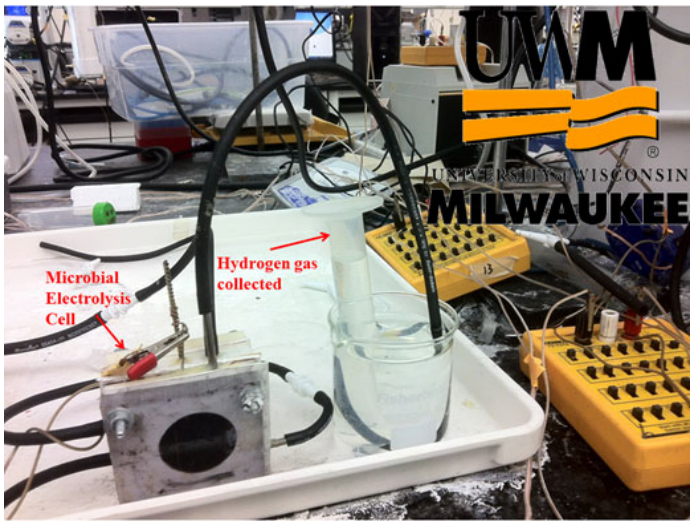

Figure S10. Photograph of hydrogen evolution from MECs.

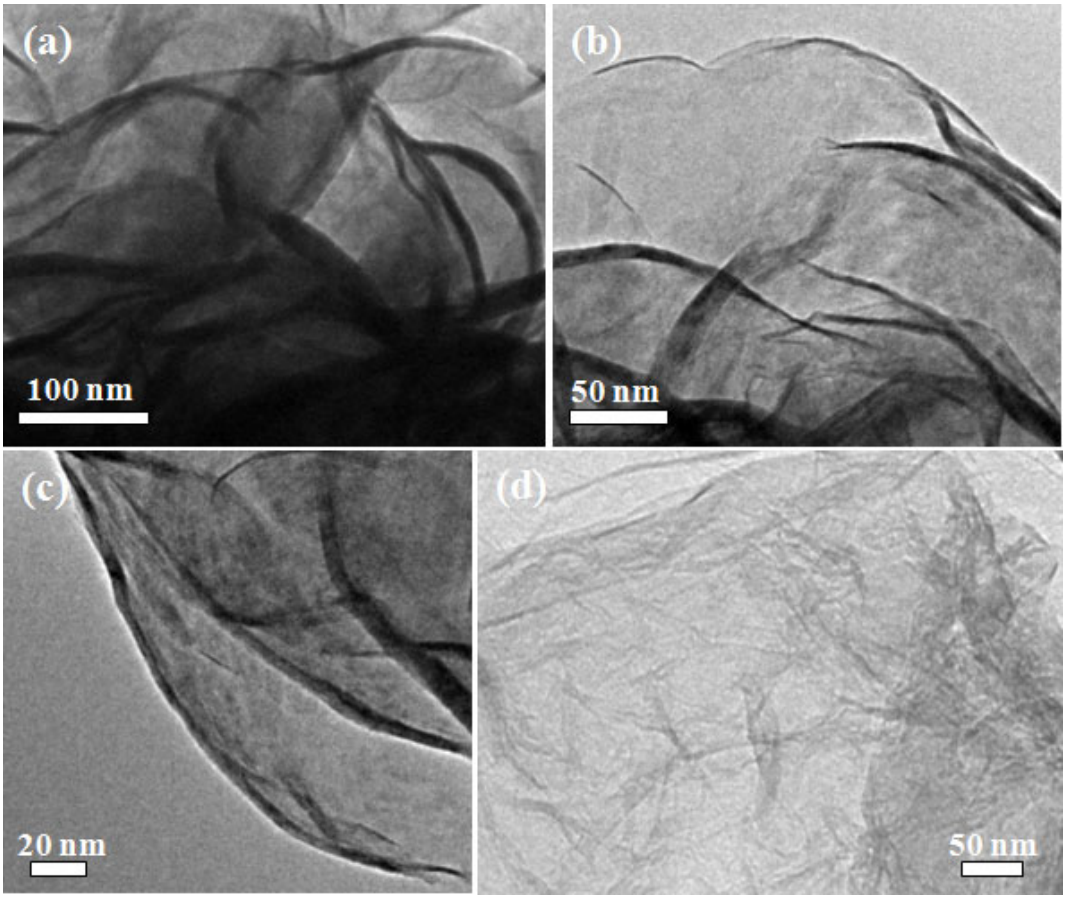

Figure S11. TEM images of MoS_2-NS (a-c) and N-GAs (d).

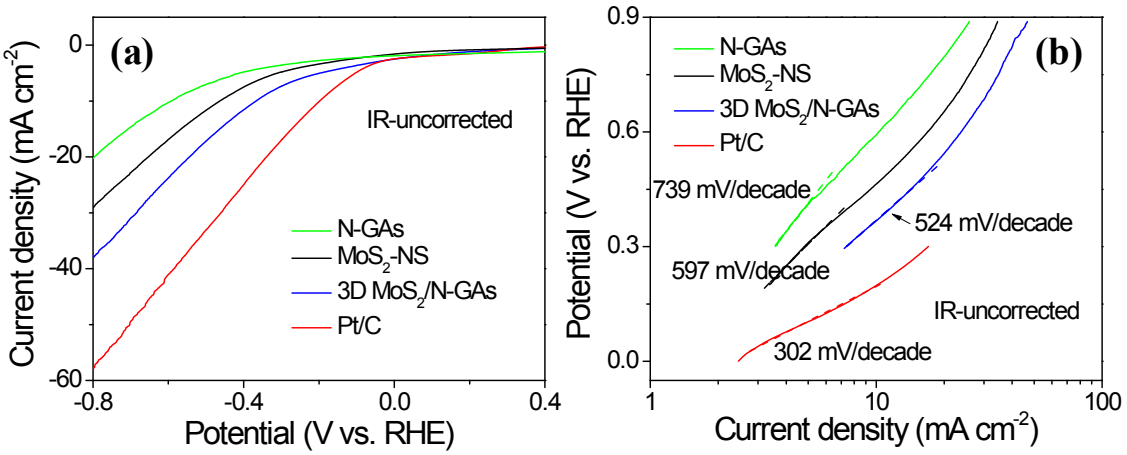

Figure S12. (a) Polarization curves and (b) corresponding Tafel plots of MoS_2-NS, N-GAs, 3D MoS_2/N-GAs, and Pt/C at 5 mV s^{-1} in 100 mM PBS. The iR drop was uncorrected.

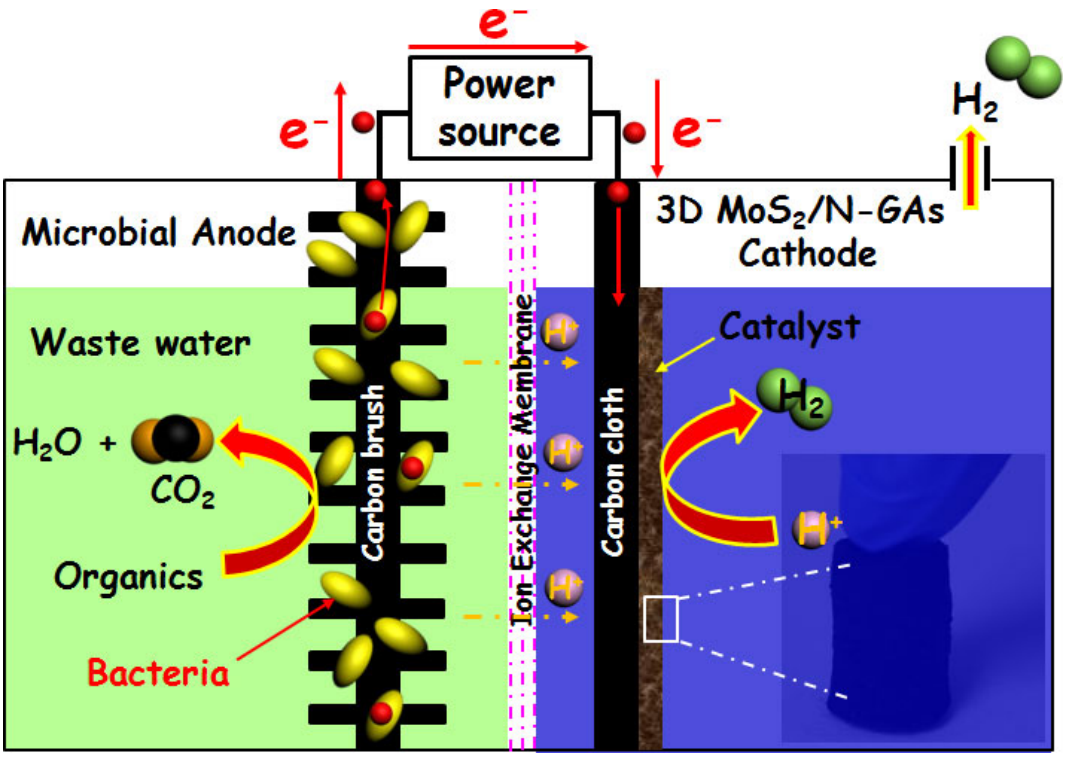

Scheme S1. Schematic diagram for the charge transfer mechanism of the 3D MoS_2/N-GAs hybrid for the MECs.

Table S1. Efficiency and hydrogen production in the MECs with different cathodes.

	Pt/C	3D MoS_2/N-GAs	MoS_2-NS	N-GAs
Coulombic Efficiency (%)	21.34±0.87	24.28±0.49	17.99±2.29	17.88±2.34
Cathodic Efficiency (%)	23.07±0.36	12.54±1.69	6.34±.72	7.07±1.65
Hydrogen Production Rate (m^3 H_2/m^3•d)	0.31±0.02	0.19±0.02	0.06±0.01	0.07±0.01

References

1 Y. Gong, S. Yang, L. Zhan, L. Ma, R. Vajtai and P. M. Ajayan, *Adv. Funct. Mater.*, 2014, **24**, 125-130.

2 W. S. Hummers and R. E. Offeman, *J. Am. Chem. Soc.*, 1958, **80**, 1339-1339.

3 Y. Hou, F. Zuo, Q. Ma, C. Wang, L. Bartels and P. Feng, *J. Phys. Chem. C*, 2012, **116**, 20132-20139.

4 Z. He, N. Wagner, S. D. Minteer and L. T. Angenent, *Environ. Sci. Technol.*, 2006, **40**, 5212-5217.

5 Y. Hou, Z. Wen, S. Cui, X. Guo and J. Chen, *Adv. Mater.*, 2013, **25**, 6291-6297.

6 C. Altavilla, M. Sarno and P. Ciambelli, *Chem. Mater.*, 2011, **23**, 3879-3885.

7 Y. Zhan, Z. Liu, S. Najmaei, P. M. Ajayan and J. Lou, *Small*, 2012, **8**, 966-971.

8 Y. Hou, T. Huang, Z. Wen, S. Mao, S. Cui and J. Chen, *Adv. Energy Mater.*, 2014, DOI: 10.1002/aenm.201400337.

9 Z. H. Sheng, L. Shao, J. J. Chen, W. J. Bao, F. B. Wang and X. H. Xia, *ACS Nano*, 2011, **5**, 4350-4358.

10 X. Xu, R. Cao, S. Jeong and J. Cho, *Nano Lett.*, 2012, **12**, 4988-4991.

11 H. Yin, C. Zhang, F. Liu and Y. Hou, *Adv. Funct. Mater.*, 2014, DOI: 10.1002/adfm.201303902.